Title	Enhancement of power conversion efficiency in solution processed organic photovoltaic devices by embedded plasmonic gold-silica core-shell nanorods
Author(s)	Xu, Xiaoyan; Wong, Terence Kin Shun; Sun, Xiao Wei
Citation	Xu, X., Wong, T. K. S., & Sun, X. W. (2014). Enhancement of power conversion efficiency in solution processed organic photovoltaic devices by embedded plasmonic gold-silica core-shell nanorods. SPIE Proceedings, 9137, 91370Z-.
Date	2014
URL	http://hdl.handle.net/10220/20080
Rights	© 2014 SPIE. This paper was published in SPIE Proceedings and is made available as an electronic reprint (preprint) with permission of SPIE. The paper can be found at the following official DOI: http://dx.doi.org/10.1117/12.2051717. One print or electronic copy may be made for personal use only. Systematic or multiple reproduction, distribution to multiple locations via electronic or other means, duplication of any material in this paper for a fee or for commercial purposes, or modification of the content of the paper is prohibited and is subject to penalties under law.

Enhancement of power conversion efficiency in solution processed organic photovoltaic devices by embedded plasmonic gold-silica core-shell nanorods

Xiaoyan Xu[a], Terence K.S. Wong*[a], Xiaowei Sun[a]
[a]School of Electrical and Electronic Engineering, Nanyang Technological University, Nanyang Avenue, Singapore 639798

ABSTRACT

Chemically synthesized gold-silica nanorods were incorporated into the active layer of solution processed organic photovoltaic devices to enhance the absorption of light by the surface plasmon resonance effect in metallic nanoparticles. Solution processed polymer:fullerene and small molecule:fullerene bulk heterojunction devices were studied. The polymer donors include regioregular poly(3-hexylthiophene) (P3HT) and low bandgap poly[2,6-(4,4-bis-(2-ethylhexyl)-4N-cyclopenta[2,1-b:3,4-b'] dithiophene)-alt-4,7-(2,1,3-benzothiadiazole)] (PCPDTBT). For the small molecule device, 7,7'-(4,4-bis(2-ethylhexyl)-4*H*-silolo[3,2-b:4,5-b']-dithiophene-2,6-diyl)bis(6-fluoro-4-(5'-hexyl-[2,2'-bithiophen]-5-yl) benzo[*c*][1,2,5]thiadiazole) (p-DTS($FBTTh_2$)$_2$) was used as the donor. The donors are blended with either [6,6]-phenyl-C_{61}-butyric acid methyl ester ($PC_{60}BM$) or [6,6]-phenyl-C_{71}-butyric acid methyl ester ($PC_{70}BM$). The gold-silica nanorods have an aspect ratio (length/diameter) of 3.2 and 2.3 and a shell thickness of ~10 nm. Prior to spin coating, the nanorods were added directly to the donor:acceptor blend solution in either chlorobenzene or dichlorobenzene at different weight percentage of the total donor:acceptor weight. The transverse and longitudinal surface plasmon resonance peaks of the gold-slica nanorods overlap with the absorption spectra of all three donor:acceptor blends to differing degrees. As a result, the power conversion efficiency of optimized plasmonic P3HT:$PC_{60}BM$ and PCPDTBT:$PC_{70}BM$ devices with conventional structure under AM1.5G illumination at 100mW/cm^2 were increased by 9.3% (to 3.42%) and 20.8% (to 4.11%) respectively relative to the control device without nanorods. For the p-DTS($FBTTh_2$)$_2$:$PC_{70}BM$ device, the relative improvement as compared to the control device was 24.2% (to 8.01%).

Keywords: nanoparticles, gold silica nanorods, core-shell, surface plasmon resonance, organic photovoltaics

1. INTRODUCTION

In recent years, there has been intense interest in applying the plasmonic properties of metallic nanoparticles to enhance the performance of organic photovoltaic (OPV) devices.[1] Due to their solution processing capability in ambient conditions and potentially low cost, OPV is a highly promising thin film photovoltaic technology. However, it is still limited by insufficient power conversion efficiency (PCE) and limited lifetime of OPV devices. In the open literature, the highest reported PCE for single junction OPV devices is approaching 9%. For commercial application, a PCE above 10% is needed. An effective approach to enhance the PCE is to increase the optical absorption in the active layer of the OPV device to increase the amount of excitons generated. The typical active layer thickness in an OPV device is of order 100nm. The active layer has to be very thin because of the short exciton diffusion length in the organic bulk heterojunction (BHJ) and low carrier mobility in organic semiconductors. As a result, the amount of light that can be absorbed in a solution deposited active layer is somewhat limited. The absorption of light in the thin active layer can be increased by the surface plasmon resonance (SPR) effect (see section 2) in noble metal nanoparticles such as gold (Au) or silver (Ag) because the SPR peaks of these metals lie in the visible region of the electromagnetic spectrum.[2] In many previous reports, spherical metallic nanoparticles were added to either the anode buffer layer or the active layer or the interface between these two layers for conjugated polymer:fullerene BHJ OPV devices.[3,4] On the other hand, there had been few studies involving non-spherical metallic nanoparticles.[5,6] In this study, we report the positive effect of incorporating Au-silica core-shell nanorods into the active layer of BHJ OPV devices comprising solution processed regioregular P3HT, low band gap PCPDTBT and (iii) small molecule p-DTS($FBTTh_2$)$_2$.

*ekswong@ntu.edu.sg; phone 65-6790-6401; fax 65-67933318; www.ntu.edu.sg

Organic Photonics VI, edited by Barry P. Rand, Chihaya Adachi, David Cheyns, Volker van Elsbergen,
Proc. of SPIE Vol. 9137, 91370Z · © 2014 SPIE · CCC code: 0277-786X/14/$18 · doi: 10.1117/12.2051717

This paper is organized as follows. In section 2, the electromagnetic theory behind the dual SPR peaks in metallic nanorods is first outlined. The experimental methods concerning OPV device fabrication and characterization are then described in section 3. The experimental results of the three BHJ OPV devices enhanced by Au-silica nanorods are discussed and compared in section 4. Finally, in section 5, we summarize the key findings of this study in the conclusion.

2. THEORY

In order to demonstrate the rationale behind our choice of Au nanorods for incorporation into the active layer of OPV devices, we first outline the plasmonic properties of metallic nanorods. As with the nanosphere, a collective oscillation of the surface conduction electrons can be excited when the frequency of incident light matches the characteristic SPR frequencies of the nanorod.[7] By extending the Mie theory originally developed for an isolated sphere, Gans showed that the extinction coefficient γ at wavelength λ for a metallic nanorod under the dipolar approximation is given by:[8]

$$\gamma(\lambda) = \frac{2\pi N V \varepsilon_m^{3/2}}{3\lambda} \sum_j \frac{\left(1/P_j^2\right)\varepsilon_2}{\left(\varepsilon_1 + \frac{1-P_j}{P_j}\varepsilon_m\right)^2 + \varepsilon_2^2} \tag{1}$$

In equation (1), ε_1 and ε_2 are the frequency dependent real and imaginary parts of the dielectric function of the nanorod material respectively; ε_m is the dielectric constant of the surrounding medium; N is the concentration of nanorods and V is the volume of each nanorod. P_j (j = A, B, C) in the summation represent the depolarization factors for the three Cartesian axes. Assuming the length of the nanorod, A parallel to the z axis is greater than the radius B and C along the x and y directions respectively:

$$P_A = \frac{1-e^2}{e^2}\left[\frac{1}{2e}\ln\left(\frac{1+e}{1-e}\right) - 1\right] \tag{2}$$

$$P_B = P_C = \frac{1}{2e^2}\left\{1 - \left(\frac{1-e^2}{2e}\right)\ln\left(\frac{1+e}{1-e}\right)\right\} \tag{3}$$

where,

$$e = \sqrt{1 - \left(\frac{B}{A}\right)^2} \tag{4}$$

For a given aspect ratio (A/B), the three depolarization factors can be found by substituting (4) into (2) and (3). The extinction coefficient γ as a function of wavelength λ can then be calculated by substituting the complex dielectric function spectrum for Au and the dielectric constant of the surrounding medium.[9] As shown by Link et. al., the theoretical extinction coefficient spectrum of Au nanorods consists of two peaks in the visible region. The peak at shorter wavelengths (around 520nm) is due to a transverse SPR mode and the peak at longer wavelengths is due to a longitudinal SPR mode. The peak positions of both the transverse and longitudinal modes are dependent on the aspect ratio. As the aspect ratio increases, the transverse mode blue shifts while the longitudinal mode red shifts. The extent of the shift for the longitudinal mode is significantly greater than that of the transverse mode. Hence, the great advantage of using Au nanorods is that the two extinction peaks can be readily tuned to match the absorption spectrum of a particular BHJ blend. This tuning property is not available with the Au nanosphere because for a sphere, the SPR peak position is not a sensitive function of the sphere radius. Since a metallic surface has high surface recombination velocity and can potentially lead to loss of photogenerated carriers, we coat the surface of the Au nanorod core with a thin silica shell to render it more suitable for incorporation into the active layer.

3. EXPERIMENT

3.1 OPV device fabrication

The OPV devices fabricated for this study all have a conventional architecture with the cathode at the top and are illuminated via the bottom substrate. A standard cleaning procedure was followed to prepare the surface of the indium tin oxide (ITO) glass with sheet resistance 15Ω/sq. The ITO glass was cleaned using de-ionized water, acetone, isopropyl alcohol with ultra-sonication and was blown dry using nitrogen gas. The ITO surface was then treated with an oxygen plasma for 3 minutes. Next, a 40nm thick layer of poly(3,4-ethylene-dioxythiophene):poly(styrenesulphonate) (PEDOT:PSS) (Baytron P 4083) was spin coated at 3000rpm for 1 minute onto the ITO. The thickness of the PEDOT:PSS was measured by profilometry. The three device structures fabricated by spin coating the active layer onto the PEDOT:PSS layer are: (i) ITO/PEDOT:PSS/P3HT:$PC_{60}BM$/Ca/Ag; (ii) ITO/PEDOT:PSS/PCPDTBT:$PC_{70}BM$/Ca/Ag and (iii) ITO/PEDOT:PSS/p- DTS$(FBTTh_2)_2$:$PC_{70}BM$/Ca/Ag.

The P3HT:$PC_{60}BM$ solution was prepared by adding a 1:0.8 mass ratio of P3HT and $PC_{60}BM$ with a combined mass of 40mg to 1ml of 1,2-dicholorobenzene (DCB). This corresponds to a concentration of 40mg/ml of DCB. The PCPDTBT:$PC_{70}BM$ blend was similarly prepared by adding 40mg of a 1:3 mass ratio of PCPDTBT and $PC_{70}BM$ to 1ml of chlorobenzene (CB) containing 10mg of the processing additive 1,8 octanedithiol (DIO). The DIO was found to be critical to improve the phase separation of the PCPDTBT:$PC_{70}BM$ blend. The p-DTS$(FBTTh_2)_2$:$PC_{70}BM$ blend was likewise obtained by adding 35 mg of p-DTS$(FBTTh_2)_2$ and $PC_{70}BM$ with a mass ratio of 3:2 to 1ml of CB containing 0.4 v/v% of DIO.

The Au-silica core-shell nanorods were synthesized following procedures reported in the literature. The Au nanorods were first prepared by a seed-mediation method. The silica shell of the Au nanorods was then synthesized by the method of Gorelikov and Matsuura. After synthesis, the Au-silica core-shell nanorods were dispersed in separate CB and DCB solvents. The reason for using two solvents is to avoid possible co-solvent effects complicating the interpretation of the device results when the Au-silica nanorods are added to the three blends above.

The P3HT:$PC_{60}BM$ blend of Au-silica nanorods was prepared by diluting the Au-silica dispersion in DCB to a concentration of 0.4mg/ml. 40mg of P3HT and $PC_{60}BM$ (1:0.8 mass ratio) was added to 1ml of this diluted solution to give a 1wt% concentration of Au-silica nanorods in the P3HT:$PC_{60}BM$ blend. For the PCPDTBT:$PC_{70}BM$ blend, 10mg of 1,8 octanedithiol (DIO) was added to 1ml of a CB dispersion of Au-silica nanorods with varying concentration. A 40mg blend of 1:3 mass ratio PCPDTBT:$PC_{70}BM$ was then added to the CB solution containing DIO and Au-silica nanorods. The reason for following this protocol is to ensure that the same amount of DIO is present in the PCPDTBT:$PC_{70}BM$ device with and without nanorods. This protocol was also followed strictly in the preparation of the p-DTS$(FBTTh_2)_2$:$PC_{70}BM$ blend with varying concentration of Au-silica nanorods. Following spin coating, a 13nm Ca interlayer and a 200nm Ag cathode layer were evaporated successively at $1x10^{-4}$ Pa onto the active layer through a metal shadow mask. The active area of the device is determined by the overlap between the metal electrode and the active layer. All devices were encapsulated with an active area of 3mm x 3mm and there are three devices per sample.

3.2 Device characterization

The morphology and dimensions of the Au-silica nanorods were characterized using a JEOL 1400 transmission electron microscope (TEM) at an accelerating voltage of 100kV. The thickness of the active layer and PEDOT:PSS layer was measured using a KLA- Tencor P-10 surface profiler. Optical absorption spectra were measured using a Perkin Elmer Lambda 950 UV/Vis/near-IR spectrophotomter equipped with a 150mm diameter integrating sphere. The absorption was obtained from the reflectance and transmittance by the equation: *absorption = 1 – reflectance – transmittance*.

The current density-voltage (*J-V*) characteristics of the OPV devices were acquired in air using a Keithley 2400 source measure unit (SMU). For *J-V* characteristics under illumination, a solar simulator (Solar Light Ltd) with a simulated AM1.5G spectrum and irradiance of $100mW/cm^2$ was used. The irradiance was calibrated using a standard silicon reference solar cell. The incident photon conversion efficiency (IPCE) spectra was measured using a Bentham PVE 300 system equipped with a xenon lamp, monochromator, light chopper and lock-in amplifier and a calibrated silicon photodetector.

4. RESULTS AND DISCUSSION

4.1 Au-silica nanorods

We synthesized two types of Au-silica core-shell nanorods using the seed-mediated method. TEM image indicates that the average length and diameter of first type of Au nanorods core are approximately 109 nm and 34 nm respectively and the thickness of the silica shell is ~10 nm (**Figure 1**). The average length and diameter of second type of Au-silica nanorods core are 92 nm and 40 nm respectively and the thickness of the silica shell are ~10 nm. The normalized UV/Vis absorption spectra reveal that Au-silica nanorods in CB have a broad absorption spectrum with dual localized SPR (LSPR) peaks at 520 nm and 733 nm for first type of Au-silica nanorods and at 520 nm and 681 nm for second type of Au-silica nanorods. This clearly shows that dual LSPR peaks can be simply adjusted by changing the aspect ratio between length and diameter of nanorod.

The major LSPR peak of nanorod at 733nm and 680 nm are well-matched with absorption peak of PCPDTBT and p-DTS(FBTTh$_2$)$_2$ respectively. Hence, we chose first type of Au-silica nanorods as plasmonic materials in polymer solar cell and second type of Au-silica nanorods in SM BHJ solar cell. Organic BHJ solar cells were fabricated with the device structure of ITO/PEDOT: PSS/Active layer/Ca/Ag as shown in **Figure 2**. The molecular structure of P3TH, PCPDTBT, p-DTS(FBTTh$_2$)$_2$, PC$_{60}$BM and PC$_{70}$BM is also shown. The Au-silica nanorods were blended directly into the BHJ.

4.2 Au-silica nanorods in P3HT:PC$_{60}$BM solar cells

The impact of Au-silica nanorods with primary LSPR at 733 nm was first studied in P3HT:PC$_{60}$BM solar cells. **Figure 3**a shows the UV-Vis absorption spectra of the P3HT:PC$_{60}$BM BHJ films with and without optimum concentration of 1 wt% Au-silica nanorods with the same thickness. The absorption spectra clearly show that the P3HT:PC$_{60}$BM film with Au-silica nanorods has more light absorption than P3HT:PC$_{60}$BM blend film in the spectral range of 300 nm to 600 nm.

To verify the light absorption enhancement originated from the LSPR of Au-silica nanorods, we conducted the *J-V* characteristics and IPCE measurements. **Figure 3**b represents the *J-V* characteristics of the P3HT:PC$_{60}$BM devices with and without 1 wt% of Au-silica nanorods under AM 1.5G irradiation at 100 mW/cm^2. The photovoltaic parameters of all prepared devices are listed in **Table 1**. The reference device has a PCE of 3.13% with an open-circuit voltage (V_{OC}) of 0.624 V, short-circuit current density (J_{SC}) of 7.99 mA/cm^2 and a fill factor (*FF*) of 62.8%. After incorporation of 1 wt% Au-silica nanorods, the maximum PCE of the device reaches to 3.42% with 9.3% enhancement. The V_{OC} remain the same while the J_{SC} increases to 8.52 mA/cm^2. Thus, improved J_{SC} indicates that light absorption is enhanced by incorporation of Au-silica nanorods. **Figure 3**c depicts the IPCE spectra of the reference device and plasmonic device with 1 wt% Au-silica nanorods. For the device with Au-silica nanorods, the IPCE increases within the wavelength range from 400 nm to 600 nm, which only match with minor absorption spectrum peak of Au-silica nanorods.

4.3 Au-silica nanorods in PCPDTBT:PC$_{70}$BM solar cells

Au-silica nanorods with primary LSPR peak at 733 nm were also adopted into PCPDTBT:PC$_{70}$BM solar cell. **Figure 4**a displays the absorption spectra of PCPDTBT:PC$_{70}$BM film with and without 1 wt% of Au-silica nanorods. It is observed that plasmonic PCPDTBT:PC$_{70}$BM film has greater optical absorption than the reference film within the spectral range from 400 nm to 800 nm. **Figure 4**b shows the *J-V* characteristics of PSCs with and without Au-silica nanorods in PCPDTBT:PC$_{70}$BM blend under 100 mW/cm^2 illumination. For the reference device, the V_{OC}, J_{SC}, *FF* and PCE are 0.597 V, 11.02 mA/cm^2, 51.7% and 3.4%, respectively. Upon incorporation of Au-silica nanorods, V_{OC} is kept same. In contrast, the J_{SC}, *FF* and PCE increase to 12.17 mA/cm^2, 56.6% and 4.11%, respectively. IPCE was also conducted to verify the enhanced J_{SC} in the PCPDTBT:PC$_{70}$BM device. **Figure 4**c shows that the IPCE spectrum of the plasmonic PCPDTBT:PC$_{70}$BM device is increased with respect to the reference device spectrum within the wavelength range from 500 nm to 800 nm. Outside this range, the two spectra are essentially overlapping. The wavelength range 500-800 nm coincides with the primary absorption spectrum peak of the Au-silica nanorods. Therefore, the PCE in PCPDTBT:PC$_{70}$BM device has larger enhancement than previous plasmonic P3HT:PC$_{60}$BM device.

4.4 Au-silica nanorods in p-DTS(FBTTh$_2$)$_2$:PC$_{70}$BM solar cells

Since p-DTS(FBTTh$_2$)$_2$ donor fulfils the requirements of a wide absorption within solar spectrum, high charge generation rate with less recombination, and good carrier transport with high and well-balanced mobilties simultaneously, Au-silica nanorods were also adopted into p-DTS(FBTTh$_2$)$_2$:PC$_{70}$BM SM solar cells. Here, the second type of Au-silica nanorods has primary LSPR peak at 681 nm which well match with the absorption spectrum of p-DTS(FBTTh$_2$)$_2$:PC$_{70}$BM. **Figure 5**a shows the absorption spectra of p-DTS(FBTTh$_2$)$_2$:PC$_{70}$BM film with and with Au-silica nanorods. The absorption increases within the spectral range from 500 nm to 700 nm after incorporating Au-silica nanorods. **Figure 5**b displays the *J-V* characteristics of the p-DTS(FBTTh$_2$)$_2$:PC$_{70}$BM devices with and without 1wt% of Au-silica nanorods under AM 1.5G irradiation at 100 mW/cm^2. For reference device, the V_{OC}, J_{SC}, FF and PCE are 0.765 V, 12.34 mA/cm^2, 68.3% and 6.45%, respectively. For plasmonic device, V_{OC} and FF have slight change. However, J_{SC} and PCE increase to 15.19 mA/cm^2 and 8.01%, respectively. Such enhancements are larger than those of P3HT:PC$_{60}$BM device and PCPDTBT:PC$_{70}$BM device. It is because that p-DTS(FBTTh$_2$)$_2$ has strong absorption within the range from 400 nm to 700 nm. **Figure 5**c shows the IPCE spectra of p-DTS(FBTTh$_2$)$_2$:PC$_{70}$BM device with and without Au-silica nanorods. IPCE spectrum of plasmonic p-DTS(FBTTh$_2$)$_2$:PC$_{70}$BM device increases from 400 nm to 700 nm which well match with the absorption spectrum of Au-silica nanorods with primary peak at 681 nm.

5. CONCLUSIONS

In summary, we demonstrate the improved the PCE of P3HT:PC$_{60}$BM device, PCPDTBT:PC$_{70}$BM device and p-DTS(FBTTh$_2$)$_2$:PC$_{70}$BM device by incorporation of Au-silica nanorods into BHJ active layer. At the concentration of 1 wt% Au-silica nanorods, PCE increased by 9.3%, 20.8% and 24.2%, respectively. Absorption spectra, *J-V* characteristics and IPCE measurements verify that the addition of Au-silica nanorods into organic solar cells leads to increased light absorption of the active layer. Better performance of Au-silica nanorods in PCPDTBT:PC$_{70}$BM device than P3HT:PC$_{60}$BM device is due to well-matched absorption spectra between PCPDTBT donor and Au-silica nanorods. While larger enhancement in p-DTS(FBTTh$_2$)$_2$:PC$_{70}$BM device than previous two devices is due to strong absorption in p-DTS(FBTTh$_2$)$_2$ donor and well-matched absorption spectra between p-DTS(FBTTh$_2$)$_2$ donor and Au-silica nanorods. The improved PCE demonstrates that the incorporation of Au-silica nanorods offers an effective way to increase the efficiency of organic solar cells.

ACKNOWLEDGEMENTS

The authors gratefully acknowledge Aung Ko Ko Kyaw, Institute of Materials Research and Engineering, Agency for Science Technology and Research, Singapore, for useful discussion.

REFERENCES

[1] Strataksi, E. and Kymakis, E., "Nanoparticle-based plasmonic organic photovoltaic devices," Mater. Today 16(4), 133-146 (2013).

[2] Tsakalakos, L, [Nanotechnology for Photovoltaics], CRC Press, Roca Baton, 391-421 (2010).

[3] Wang, D.H., Kim, D.Y., Choi, K.W., Seo, J.H., Im, S.H., Park, J.H., Park, O.O. and Heeger, A.J., "Enhancement of donor-acceptor polymer bulk heterojunction solar cell power conversion efficiency by addition of Au nanoparticles," Angew. Chem. 123, 5633-5637 (2011).

[4] Wu, J.L., Chen, F-C., Hsiao, Y-S., CHien, F-C., Chen, P., Kuo, C-H., Huang, M.H. and Hsu, C-S., "Surface plasmonic effects of metallic nanoparticles on the performance of polymer bulk heterojunction solar cells," ACS Nano 2, 959-967 (2011).

[5] Wang, D.H., Kim, J.K., Lim, G-H., Park, K.H., Park, O.O., Lim, B. and Park, J.H., "Enhanced light harvesting in bulk heterojunction photovoltaic devices with shape-controlled Ag nanomaterials: Ag nanoparticles *versus* Ag nanoplates," RSC Advances 2, 7268-7272 (2012).

[6] Kim, C-H. Cha, S-H., Kim, S.C., Song, M., Lee, J., Shin W.S., Moon, S-J., Bahng, J.H., Kotov, N.A. and Jin, S-H., "Silver nanowire embedded in P3HT:PCBM for high-efficiency hybrid photovoltaic device applications," ACS Nano 4, 3319-3325 (2011).

[7] Louis, C. and Pluchery, O., [Gold Nanoparticles for Physics, Chemistry and Biology], Imperial College Press, London, 43-74 (2012).

[8] Link, S., Mohamed, M.B. and El-Sayed, M.A., "Simulation of the optical absorption spectra of gold nanorods as a function of their aspect ratio and the effect of the medium dielectric constant," J. Phys. Chem. B 103, 3073-3077 (1999).

[9] Johnson, P.B. and Christy, R.W., "Optical constants of noble metals," Phys. Rev. B 6(12), 4370-4379 (1972).

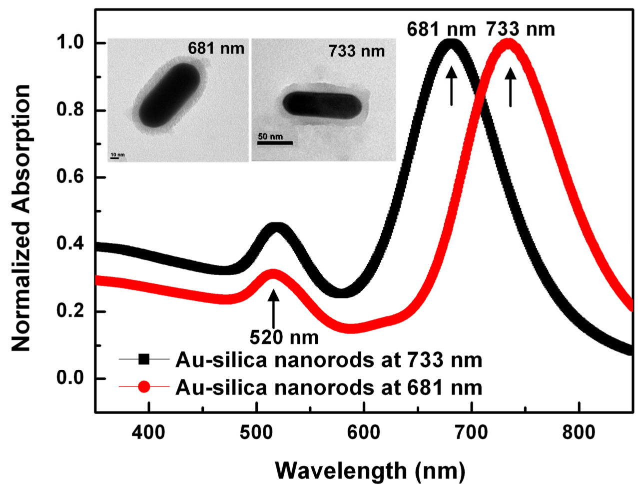

Figure 1 Normalized UV-Vis absorption spectra of two types of Au–silica nanorods with the surface plasmon resonance peaks at 681 nm and 733 nm respectively. The inset is the TEM image of corresponding Au-silica nanorods. The scale bar represents 10 nm and 50 nm respectively.

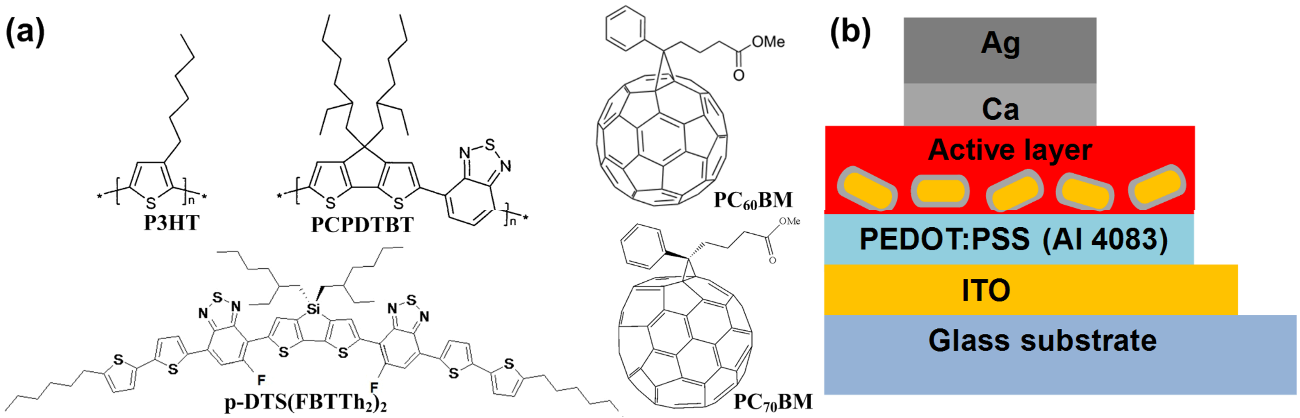

Figure 2 (a) Molecular structures of the P3HT, PCPDTBT, $PC_{60}BM$, p-DTS$(FBTTh_2)_2$ and $PC_{70}BM$ and (b) device structure of organic solar cell.

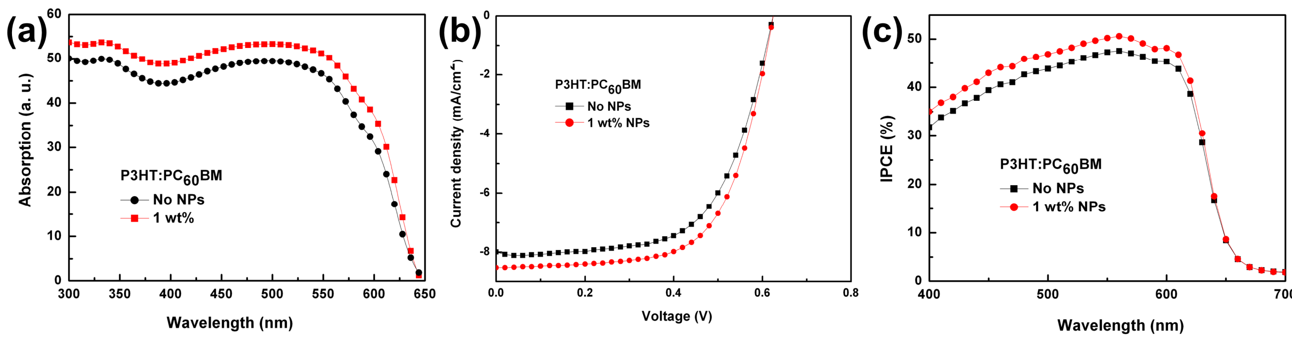

Figure 3 (a) UV-Vis absorption spectra of P3HT:PC_{60}BM BHJ films with and without NPs, (b) *J-V* characteristics of P3HT:PC_{60}BM solar cells with and without NPs and (c) IPCE spectra of P3HT:PC_{60}BM solar cells with and without NPs.

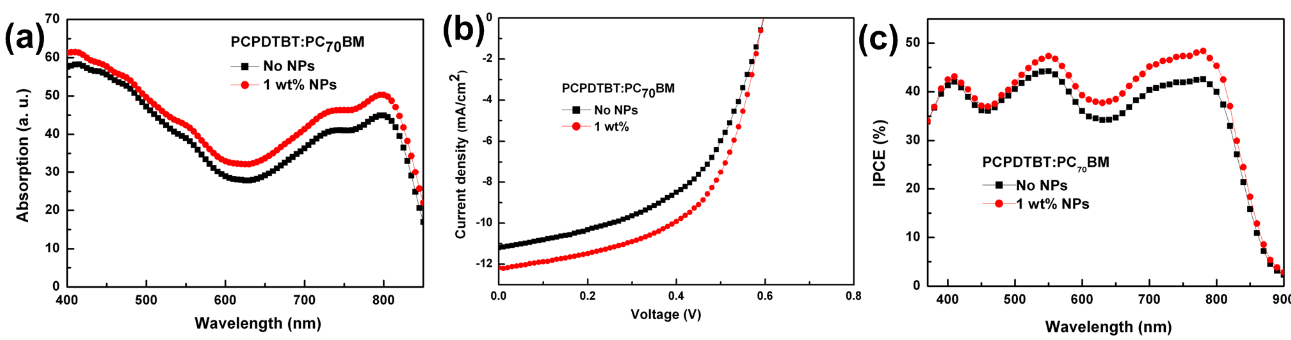

Figure 4 (a) UV-Vis absorption spectra of PCPDTBT:PC_{70}BM BHJ films with and without NPs, (b) *J-V* characteristics of PCPDTBT:PC_{70}BM solar cells with and without NPs and (c) IPCE spectra of PCPDTBT:PC_{70}BM BHJ solar cells with and without NPs.

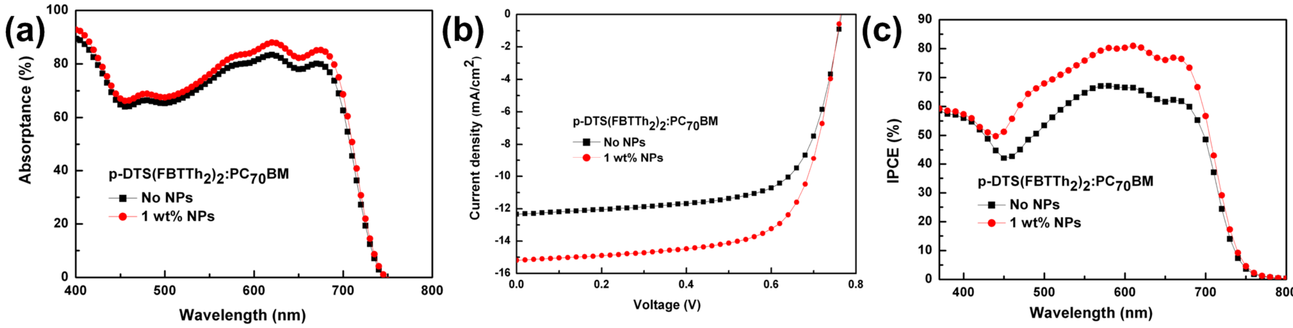

Figure 5 (a) UV-Vis absorption spectra of p-DTS$(FBTTh_2)_2$:$PC_{70}BM$ BHJ films with and without NPs, (b) *J-V* characteristics of p-DTS$(FBTTh_2)_2$:$PC_{70}BM$ solar cells with and without NPs and (c) IPCE spectra of p-DTS$(FBTTh_2)_2$:$PC_{70}BM$ BHJ solar cells with and without NPs.

Table 1 Device performance parameters of different organic solar cells with and without Au-silica nanorods under 100 mW/cm^2 AM 1.5G simulated solar irradiation.

Device	V_{oc}(V)	J_{sc} (mA/cm^2)	*FF* (%)	PCE (%)
P3HT:$PC_{60}BM$	0.624	7.99	62.8%	3.13%
P3HT:$PC_{60}BM$ with NPs	0.624	8.52	64.3%	3.42%
PCPDTBT:$PC_{70}BM$	0.597	11.02	51.7%	3.40%
PCPDTBT:$PC_{70}BM$ with NPs	0.595	12.17	56.6%	4.11%
p-DTS$(FBTTh_2)_2$:$PC_{70}BM$	0.765	12.34	68.3%	6.45%
p-DTS$(FBTTh_2)_2$:$PC_{70}BM$ with NPs	0.763	15.19	69.1%	8.01%